Developmental Biology 340 (2010) 306–317

Contents lists available at ScienceDirect

Developmental Biology

journal homepage: www.elsevier.com/developmentalbiology

Genomes & Developmental Control

The Hox cofactors Meis1 and Pbx act upstream of *gata1* to regulate primitive hematopoiesis

Laura M. Pillay [a], A. Michael Forrester [c,e], Timothy Erickson [a], Jason N. Berman [c,e], Andrew Jan Waskiewicz [a,b,d,*]

[a] Department of Biological Sciences, University of Alberta, Edmonton, Canada
[b] Centre for Neuroscience, University of Alberta, Edmonton, Canada
[c] Department of Pediatrics, IWK Health Centre, Dalhousie University, Halifax, Canada
[d] Women and Children's Health Research Institute, University of Alberta, Edmonton, Canada
[e] Department of Microbiology/Immunology, IWK Health Centre, Dalhousie University, Halifax, Canada

ARTICLE INFO

Article history:
Received for publication 11 September 2009
Revised 26 January 2010
Accepted 26 January 2010
Available online 1 February 2010

Keywords:
Pbx
Meis
Meis1
Gata1
Hematopoiesis
Zebrafish
Hox
Hoxb7a
Cdx
Lmo2
Hemoglobin
Scl
Erythropoiesis
Erythroid
Myeloid
Myelopoiesis
Pu.1
Spi1

ABSTRACT

During vertebrate development, the initial wave of hematopoiesis produces cells that help to shape the developing circulatory system and oxygenate the early embryo. The differentiation of primitive erythroid and myeloid cells occurs within a short transitory period, and is subject to precise molecular regulation by a hierarchical cascade of transcription factors. The TALE-class homeodomain transcription factors Meis and Pbx function to regulate embryonic hematopoiesis, but it is not known where Meis and Pbx proteins participate in the hematopoietic transcription factor cascade. To address these questions, we have ablated Meis1 and Pbx proteins in zebrafish, and characterized their molecular effects on known markers of primitive hematopoiesis. Embryos lacking Meis1 and Pbx exhibit a severe reduction in the expression of *gata1*, the earliest marker of erythroid cell fate, and fail to produce visible circulating blood cells. Concomitant with a loss of *gata1*, Meis1- and Pbx-depleted embryos exhibit downregulated embryonic hemoglobin (*hbae3*) expression, and possess increased numbers of *pu.1*-positive myeloid cells. *gata1*-overexpression rescues *hbae3* expression in Pbx-depleted; *meis1*-morphant embryos, placing Pbx and Meis1 upstream of *gata1* in the erythropoietic transcription factor hierarchy. Our study conclusively demonstrates that Meis1 and Pbx act to specify the erythropoietic cell lineage and inhibit myelopoiesis.

Introduction

Primitive hematopoiesis influences morphology of the developing embryonic circulatory system (Baumann and Dragon, 2005; Hove et al., 2003) and produces circulating erythrocytes that facilitate tissue oxygenation during periods of rapid embryonic growth (Orkin and Zon, 2008). Analyses in vertebrate models have identified a cascade of transcription factors that are critical for the specification of primitive erythrocytes. However, the upstream mechanisms by which these factors are regulated remain largely unclear. Previous research has shown that overexpressing posteriorly-expressed *hox* genes partially rescues erythropoietic gene expression in mutants with defects in primitive blood cell differentiation (Davidson et al., 2003; Davidson and Zon, 2006). These data support a model whereby Hox transcription factors serve to regulate primitive hematopoiesis. The Hox cofactors Meis1 and Pbx have also been implicated in hematopoiesis; *Pbx1*-knockout and *Meis1*-deficient mice exhibit profound embryonic anemia (Azcoitia et al., 2005; DiMartino et al., 2001; Hisa et al., 2004). Notably, the precise molecular function of Meis1 and Pbx in regulating primitive hematopoiesis remains to be elucidated, and it is not yet known where Meis1 and Pbx participate in the hematopoietic transcription factor hierarchy. In the present work, we analyze the

* Corresponding author. CW405, Biological Sciences Building, University of Alberta, Edmonton, Alberta, Canada T6G 2E9. Fax: +1 780 492 9234.
E-mail address: aw@ualberta.ca (A.J. Waskiewicz).

0012-1606/$ – see front matter © 2010 Elsevier Inc. All rights reserved.
doi:10.1016/j.ydbio.2010.01.033

function of Meis1 and Pbx by ablating these proteins and characterizing their molecular effects on known regulators of zebrafish primitive hematopoiesis.

Several lines of evidence suggest that Hox transcription factors act as master regulators of hematopoietic cell fate decisions (Abramovich and Humphries, 2005). Mice bearing deletions in *Hoxb3*, *Hoxb4*, *Hoxb6*, *Hoxa7*, *Hoxc8*, and/or *Hoxa9* possess defects in the development of multiple hematopoietic lineages (Brun et al., 2004; Izon et al., 1998; Kappen, 2000; Ko et al., 2007; Lawrence et al., 1997; Magnusson et al., 2007a; Shimamoto et al., 1999; So et al., 2004). In zebrafish, *hoxb6b*, *hoxb7a*, and *hoxa9a* regulate primitive erythropoiesis and contribute to hematopoietic stem cell formation (Davidson et al., 2003; Davidson and Zon, 2006). *Hox* genes are also implicated as proto-oncogenes in hematological malignancies (Kroon et al., 2001; Nakamura et al., 1996; Pineault et al., 2003; Slape and Aplan, 2004). The specificity of Hox proteins is achieved through their interaction with other DNA-binding cofactors (Mann, 1995; Mann and Affolter, 1998; Mann and Chan, 1996). Such cofactors include the Three Amino acid Loop Extension (TALE)-class homeodomain transcription factors Meis (Myeloid Ecotropic Integration Site), Pbx (Pre-B-Cell Leukemia Homeobox), and Prep/PKnox (Pbx Knotted Homeobox). Meis/Prep and Pbx coordinately bind DNA with Hox proteins, increasing their DNA-binding affinity as well as specificity (Berthelsen et al., 1998a; Chan and Mann, 1996; Chan et al., 1996; Chang et al., 1997; Ebner et al., 2005; Knoepfler et al., 1996; LaRonde-LeBlanc and Wolberger, 2003; Mann, 1995; Mann and Chan, 1996). Embryos lacking Meis and Pbx display phenotypes that are consistent with a total lack of Hox function. For example, loss of both Pbx2 and Pbx4 in the zebrafish hindbrain generates an anteriorizing homeotic transformation of the neural tube, in which rhombomeres 2–6 take on the molecular and neuronal identity of rhombomere 1 (Popperl et al., 2000; Waskiewicz et al., 2002). A nearly identical phenotype results from the knockdown of *Hoxa1*, *Hoxb1*, and *Hoxd1* gene products in *Xenopus* (McNulty et al., 2005). In zebrafish, overexpressing *meis3* in combination with *pbx4* and *hoxb1b* posteriorizes the neural tube, transforming the presumptive forebrain and midbrain regions into a hindbrain fate (Vlachakis et al., 2001). Combined, these data illustrate the significant role that TALE-class proteins play as Hox cofactors *in vivo*. It should be noted that Pbx and Meis/Prep1 proteins also form stable heterodimeric complexes in the absence of Hox proteins (Berthelsen et al., 1998b; Chang et al., 1997; Rieckhof et al., 1997), and are regulated both pre- and post-transcriptionally. For example, Meis1 is normally sequestered in the cytoplasm, but Pbx–Meis complexes are actively transported into the nucleus (Abu-Shaar et al., 1999; Berthelsen et al., 1999; Jaw et al., 2000; Mercader et al., 1999; Rieckhof et al., 1997; Vlachakis et al., 2001). Meis and Pbx proteins also bidirectionally stabilize each other. This stabilization is dependent upon domains that mediate Meis–Pbx complex formation (Jaw et al., 2000; Longobardi and Blasi, 2003; Waskiewicz et al., 2001).

In addition to their role in hindbrain patterning, there is evidence that TALE-class proteins also play an important role in the regulation of embryonic hematopoiesis. *Pbx1*-knockout mice display a lethal reduction in definitive multipotent blood progenitors, leading to reduced hematocrit and severe embryonic anemia (DiMartino et al., 2001). *Meis1*-deficient mice display a severe reduction in myeloerythroid progenitors (Azcoitia et al., 2005; Hisa et al., 2004), and *Prep1*-deficient mice exhibit profound anemia (Di Rosa et al., 2007; Ferretti et al., 2006; Penkov et al., 2005). Although these studies demonstrate a strong correlation between Hox cofactor function and hematopoiesis, they fail to elucidate the precise molecular function of Meis and Pbx during blood cell differentiation.

In the present study, we provide evidence that Meis and Pbx proteins are essential regulators of zebrafish primitive hematopoiesis. We demonstrate that inhibiting zebrafish Meis1 and Pbx protein synthesis cripples the production of circulating erythrocytes, and generates defects in erythropoietic gene expression. We also demonstrate that Meis–Pbx complexes are required for proper expression of *gata1*, but are not required to initiate *scl* expression. This phenotype is strikingly different from that of a *cdx4*/*cdx1*-depleted zebrafish embryo, which completely lacks early *scl* expression. We propose a model placing Meis1 and Hox downstream of Cdx, and upstream of *gata1* in the molecular hierarchy of primitive hematopoiesis.

Materials and methods

Zebrafish strains, genotyping, and morpholinos

The b557 allele of *pbx4* (also known as *lazarus* or *lzr*) was originally identified through the altered hindbrain expression pattern of *egr2b* (*krox20*), as previously described (Popperl et al., 2000). Pbx-depleted embryos were generated by injecting one-cell stage embryos from a heterozygous mutant *lzr*$^{+/-}$ (*pbx4*$^{+/-}$) incross with a combination of the following four previously described Pbx translation-blocking morpholinos:

pbx2-MO1, CCGTTGCCTGTGATGGGCTGCTGCG (1 ng);
pbx2-MO2, GCTGCAACATCCTGAGCACTACATT (2 ng);
pbx4-MO1, AATACTTTTGAGCCGAATCTCTCCG (3 ng);
pbx4-MO2, CGCCGCAAACCAATGAAAGCGTGTT (3 ng) (Erickson et al., 2007).

This method yields 75% Pbx-depleted embryos (*lzr*$^{+/-}$ and *lzr*$^{-/-}$) and 25% partially-depleted embryos (*lzr*$^{+/+}$). The effectiveness of this approach at removing >95% of total Pbx protein has been documented using a pan-Pbx antibody (Maves et al., 2007; Waskiewicz et al., 2002). Pbx-depleted embryos are phenotypically indistinguishable from maternally and zygotically mutant *lzr* embryos injected with *pbx2* morpholinos, and were identified through *in situ* hybridization assays for the downregulation of *eng2a* (Erickson et al., 2007) and abrogation of *egr2b* (*krox20*) expression (Popperl et al., 2000; Waskiewicz et al., 2002).

Meis1-deficient embryos were generated by injecting one-cell AB embryos with 4 ng of translation-blocking *meis1* morpholino; GTATATCTTCGTACCTCTGCGCCAT, as previously described (French et al., 2007). The specificity of this morpholino was assessed through the observation of expected hindbrain phenotypes (French et al., 2007), mRNA rescue experiments (French et al., 2007), and immunohistochemical analysis of Meis1 protein levels using the P2A6 monoclonal antibody (Fig. 3).

Gata1-deficient embryos were generated by injecting one-cell AB embryos with 5 ng of translation-blocking *gata1* morpholino; CTGCAAGTGTAGTATTGAAGATGTC, as previously described (Galloway et al., 2005).

Cdx-depleted embryos were generated by injecting one-cell *cdx4* $^{-/-}$ (*kgg*^{tv205}) embryos with 5 ng of translation-blocking *cdx1a* morpholino; CAGCAGATAGCTCACGGACATTTTC, as previously described (Davidson and Zon, 2006).

Whole-mount in situ hybridization and histochemical staining

Examination of gene expression by whole-mount *in situ* hybridization was performed essentially as previously described (French et al., 2009; Gongal and Waskiewicz, 2008). Proteinase K treatment (10 μg/ml) was performed for 30 s (12 to 16 hpf embryos) and 3 min (24 hpf embryos). Two-color *in situ* and histochemical staining of hemoglobin by o-dianisidine (Sigma) were preformed as previously described (Erickson et al., 2007; Lieschke et al., 2001).

Embryos were photographed using a Zeiss AxioImager Z1 compound microscope with an Axiocam HR digital camera under a 10× objective, using an Olympus stereoscope with a QImaging micropublisher camera, or using a Leica stereoscope with a Leica

DFC420C camera. Images were assembled in Photoshop (Adobe). Embryos were raised at 25–33 °C and staged according to published morphological hallmarks (Kimmel et al., 1995).

Quantitative real-time PCR

RNA was extracted from 50–100 16 hpf embryos using RNAqueous-4PCR (Ambion) according to manufacturer's specifications. First-strand cDNA synthesis was performed using the AffinityScript QPCR cDNA Synthesis Kit (Stratagene), with random primers, according to manufacturer's specifications. cDNA was analyzed with Brilliant SYBR Green QPCR Master Mix (Stratagene) by quantitative real-time PCR, using the StepOnePlus Real-Time PCR System (Applied Biosystems). All samples were run in replicates of nine, and each experiment was repeated twice. The PCR cycle conditions were 95 °C for 10 min, (95 °C for 30 s, 55 °C for 1 min, and 72 °C for 30 s) for 40 cycles. Fluorescence readings were taken after the 55 °C annealing step. The Ct value data were analyzed using the comparative Ct method ($2^{-\Delta\Delta Ct}$ method) (Livak and Schmittgen, 2001).

Intron-spanning *gata1* and *elongation factor 1-alpha* (*ef1a*) primers were selected from the Universal Probe Library Assay Design Center for Zebrafish (Roche). Prior to cDNA analysis, primer sets were validated. For each primer set, an amplification plot was produced from a standard cDNA 2-fold dilution series. This plot was used to generate a linear regression curve. Both *gata1* (test) and *ef1a* (endogenous control) primer sets were shown to produce linear regression slopes of -3.3 ± 0.1 with a coefficient of determination (R^2) of 0.99. The *ef1a* primers produce a slope within 0.1 of the *gata1* primer set slope. PCR primer sequences are *gata1*-F, GAGACTGACCTACTGCCATCG; *gata1*-R, TCCCAGAATTGACTGAGATGAG; *ef1a*-F, CCTTCGTCCCAATTTCAGG; *ef1a*-R, CCTTGAACCAGCCCATGT.

mRNA constructs

All mRNAs were transcribed from linearized templates using the mMessage mMachine kit (Ambion) according to manufacturer's specifications. Once synthesized, mRNAs were purified using YM-50 Microcon columns (Amicon, Millipore), their concentrations determined via spectrophotometry, and diluted in DEPC-treated water. To make N-terminal 3× FLAG-tagged *hoxb7a* mRNA, a full-length *hoxb7a* ORF was cloned into the FLAG-T7TS expression vector. To make N-terminal 6× Myc-tagged *gata1* mRNA, a full-length *gata1* ORF was cloned into the pCS2+MT expression vector. The constructs pCS2+MT-*pbx4* and pCS3+MT-*meis1* were described previously (Popperl et al., 2000; Waskiewicz et al., 2001). The following amounts of mRNAs were injected into single-cell embryos: *hoxb7a* mRNA, 50 pg; *gata1* mRNA, 20 pg; *pbx4* mRNA, 200 pg; and *meis1* mRNA, 200 pg.

Immunohistochemistry

Meis1 monoclonal antibody staining was performed using 4% paraformaldehyde (PFA)/phosphate-buffered saline (PBS)-fixed embryos, 14 hpf embryos were permeabilized (5 min in 10 µg/ml Proteinase K/PBST), blocked (PBS + 0.1% Triton X-100 + 1% Bovine Serum Albumin (BSA) + 5% goat serum) for 1 h, and incubated in a 1/5 dilution of P2A6 hybridoma supernatant/block overnight at 4 °C. Embryos were washed, reblocked, and incubated overnight at 4 °C in a 1/500 dilution of Alexa Fluor 488-conjugated goat anti-mouse secondary antibody (Molecular Probes). Embryonic nuclei were stained with Hoechst 33258 (Molecular Probes), which was assigned a false color (red). Embryos were washed, deyolked, cleared in 70% glycerol, mounted, and visualized under a 10× objective (Fig. S3) or a 100× objective (Fig. 3) using a Leica TCS-SP2 spectral confocal microscope.

Results

Loss of Meis1 results in the production of erythropoietic defects

meis1 is expressed broadly in the posterior mesoderm and intermediate cell mass (ICM) during primitive hematopoiesis (Minehata et al., 2008; Waskiewicz et al., 2001). To assess the requirement for Meis1 in zebrafish primitive hematopoiesis, we generated embryos that lack Meis1 protein (hereafter called *meis1*-morphants). *meis1*-morphant embryos possess fewer visible circulating blood cells than their wild type counterparts at 48 hours post fertilization (hpf), and 67% ($n = 181$) of *meis1*-morphant embryos fail to produce any visible circulating blood cells by 48 hpf (Figs. 1A, B). Furthermore, *meis1*-morphant embryos also display a severe reduction in the number of differentiated erythrocytes, as visualized through o-dianisidine staining of 48 hpf embryos (Figs. 1C, D).

In order to determine if Meis1 is required to initiate hematopoietic gene expression, we compared the expression of *scl*, *lmo2*, *gata1*, and *flk1a* in the posterior lateral-plate mesoderm (PLM) of 16 hpf wild type and *meis1*-morphant embryos. *meis1*-morphant embryos exhibit reduced expression of the erythroid precursor marker *gata1* (Figs. 2A, A'), but maintain near normal expression of the endothelial marker *flk1a* (Figs. 2B, B'), as shown through *in situ* hybridization. These data suggest that Meis1 regulates early erythroid-specific gene expression. *scl* and *lmo2* are expressed in a region of the PLM that gives rise to both blood and endothelial precursors (Dooley et al., 2005; Gering et al., 1998, 2003; Patterson et al., 2007). Although the overall level of *lmo2* and *scl* expression is near normal in 16 hpf *meis1*-morphant embryos, the lateral-most domain of expression is reduced or absent (Figs. 2C–D'; arrowheads). In wild type embryos, this lateral domain of *scl* expression colocalizes with the pronephric mesoderm marker *pax2a* (Fig. S1; arrowheads), suggesting that it gives rise to kidney progenitor cells.

We next examined *scl*, *lmo2*, and *gata1* expression at 24 hpf to determine if Meis1 is required to maintain hematopoietic gene expression. By 24 hpf, approximately 1 h prior to the initiation of circulation, *meis1*-morphant embryos exhibit reduced hematopoietic gene expression in the ICM, as shown through *in situ* hybridization (Figs. 2E–G'). In comparison to wild type embryos, *meis1*-morphant embryos demonstrate decreased *gata1* (Fig. 2E'), *scl* (Fig. 2F'), and *lmo2* (Fig. 2G') expression, but display normal expression of the erythroid cell marker *draculin* (*drl*; data not shown).

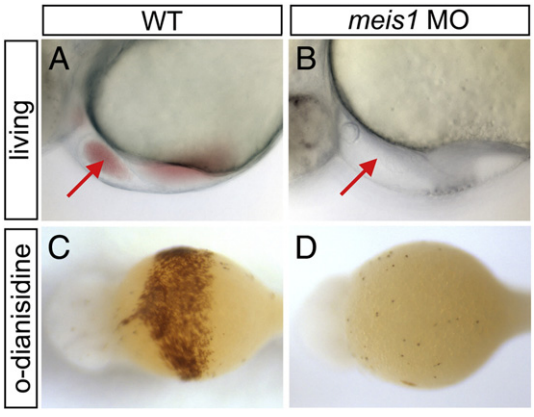

Fig. 1. *meis1*-morphant embryos fail to produce visible circulating erythrocytes. (A, B) Lateral view of live 48 hpf embryos showing close-up of heart region; anterior to the left. Unlike their wild type (WT) counterparts (A), *meis1*-morphant (B) embryos lack visible circulating blood cells. Arrows indicate heart. (C, D) o-dianisidine staining of differentiated erythrocytes in 48 hpf whole-mount embryos; ventral view with anterior to the left. o-dianisidine staining is abolished in *meis1*-morphant (D) embryos when compared to WT embryos (C).

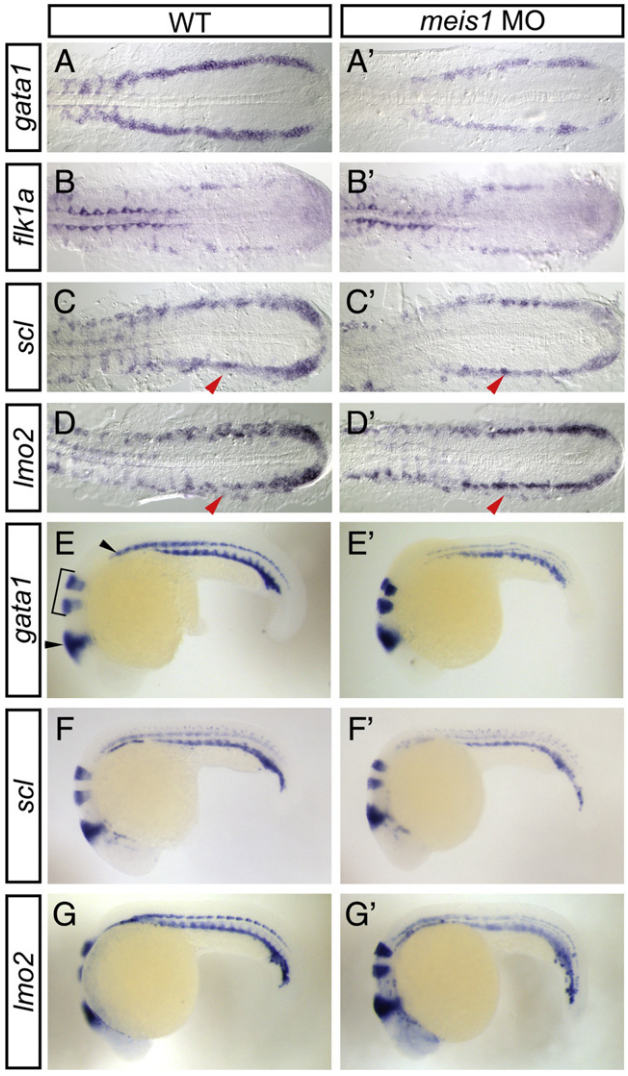

Fig. 2. *meis1*-morphant embryos exhibit defects in primitive hematopoietic gene expression. Shown are representative embryos following *in situ* hybridization analysis of hematopoietic marker expression in wild type (WT; A–G) compared with *meis1*-morphant (A'–G') embryos. (A–D') The PLM of 16 hpf flat-mounted, deyolked embryos is shown in dorsal view with anterior to the left. *gata1* expression is severely reduced in *meis1*-morphant embryos (A'; 85%, $n=39$) when compared to WT (A). *flk1a* expression is unchanged in *meis1*-morphant embryos (B'; 100%, $n=21$) when compared to WT (B). Lateral domain of *scl* (90%, $n=29$) and *lmo2* expression (79%, $n=24$) is abolished in *meis1*-morphant embryos (C′, D′; red arrowheads), while the medial domain of *scl* and *lmo2* expression is near normal. (E–G′) 24 hpf whole-mount embryos are shown in lateral view with anterior to the left. *eng2a* expression in the midbrain hindbrain boundary and muscle pioneers (E; black arrowheads) and *egr2b* expression in hindbrain rhombomeres 3 and 5 (E; bracket) is shown in all panels. *gata1* (E′; 91%, $n=53$), *scl* (F′; 97%, $n=35$), and *lmo2* (G′; 92%, $n=36$) expression is reduced in the lCM of *meis1*-morphant embryos when compared to WT (E–G).

Pbx stabilizes Meis1 and is required for its nuclear localization

Meis1 forms stable heterodimeric complexes with the TALE-class homeodomain protein Pbx (Berthelsen et al., 1998b; Chang et al., 1997; Rieckhof et al., 1997). Of the zebrafish *pbx* genes, only *lazarus* (*lzr*/*pbx4*) and *pbx2* are expressed ubiquitously in the PLM and ICM during primitive hematopoiesis (Maves et al., 2007; Popperl et al., 2000; Vlachakis et al., 2001; Waskiewicz et al., 2002). To assess the requirement for Pbx in zebrafish primitive hematopoiesis, we generated embryos that are deficient for both Pbx2 and Pbx4 (hereafter referred to as Pbx-depleted). Like *meis1*-morphants, Pbx-depleted embryos possess fewer visible circulating blood cells than their wild type counterparts at 48 hpf, and 45% ($n=66$) of Pbx-depleted embryos fail to produce any visible circulating blood cells by 48 hpf (data not shown). Furthermore, Pbx-depleted and *meis1*-morphant embryos exhibit nearly identical defects in primitive hematopoietic gene expression, as shown through *in situ* hybridization (Fig. S2).

Given the phenotypes that *meis1*-morphant and Pbx-depleted embryos share with regards to hematopoietic gene expression, we wanted to investigate further the relationship between these two heterodimeric partners. In zebrafish, overexpressing *pbx4* generates an increase in Meis1 protein levels (Waskiewicz et al., 2001). In a reciprocal fashion, overexpressing *meis1* generates an increase in Pbx4 protein levels (Waskiewicz et al., 2001). This bidirectional stabilization is dependent upon the N-terminal MH domain of Meis1, and the PBC domains of Pbx4 (Waskiewicz et al., 2001), the exact domains that mediate Pbx4–Meis1 heterodimer formation (Knoepfler et al., 1997). This stabilization is observed following the injection of mRNA constructs (Waskiewicz et al., 2001), suggesting that it occurs post-transcriptionally. Given this stabilization phenotype, it is plausible that Pbx-depleted and *meis1*-morphant embryos each possess reduced levels of Meis1 protein. To test this hypothesis *in vivo* under conditions where neither protein is overexpressed, we examined Meis1 protein levels in 14 hpf wild type and Pbx-depleted zebrafish embryos through immunohistochemical staining with the P2A6 anti-Meis1 monoclonal antibody. At 14 hpf, this antibody stains nuclei in a tissue-specific pattern that is consistent with *meis1* mRNA expression (Fig. S3). P2A6 antibody staining is nearly abolished in *meis1*-morphants (Fig. 3D), and is rescued by *meis1*-overexpression (data not shown). Combined, these data suggest that the P2A6 antibody specifically labels Meis1 protein. In the PLM of 14 hpf wild type embryos, anti-Meis1 antibody staining is punctate and colocalizes with Hoechst nuclear staining (Figs. 3A–C), indicating that Meis1 is present primarily within the nucleus. Conversely, Pbx-depleted embryos exhibit extremely low levels of anti-Meis1 antibody staining in the PLM at 14 hpf (Fig. 3G). In Pbx-depleted embryos, this low level of anti-Meis1 antibody staining does not colocalize with Hoechst nuclear staining (Figs. 3G–I), indicating that Meis1 is predominantly excluded from the nucleus. As Pbx-depletion and *meis1*-morpholino injection does not fully eliminate anti-Meis1 antibody staining, we next sought to combine these manipulations in order to generate a more complete loss of Meis1 protein. As predicted, Pbx-depleted; *meis1*-morphant embryos (Fig. 3J) display less anti-Meis1 antibody staining than *meis1*-morphant (Fig. 3D) or Pbx-depleted (Fig. 3G) embryos. Combined, these data suggest that Meis1 requires Pbx for its nuclear localization and stabilization *in vivo*.

Effects of combined Meis1 and Pbx knockdown

Given that the simultaneous depletion of Pbx and Meis1 generates a more profound effect on Meis1 protein levels than through removal of either protein alone, we next sought to investigate erythropoietic gene expression in Pbx-depleted; *meis1*-morphant embryos. To do this, we examined the expression of *gata1* and *hbae3* in the PLM of 16 hpf embryos lacking both Pbx and Meis1. In comparison to wild type embryos, embryos partially depleted of Pbx or Meis1 (injected with a half-dose of *pbx2/4* MO or *meis1* MO respectively) exhibit subtle decreases in *gata1* and *hbae3* erythroid gene expression at 16 hpf, as shown through *in situ* hybridization (Figs. 4A–C, E–G). Embryos partially depleted of both Pbx and Meis1 exhibit a severe decrease in *gata1* expression (Fig. 4D) and nearly abolished *hbae3* expression (Fig. 4H), defects that are more severe than through knockdown of either protein alone.

To measure quantitatively the observed changes in *gata1* expression, we performed real-time quantitative PCR on 16 hpf wild type embryos, *lzr*/*pbx4*$^{+/-}$ incross progeny injected with *pbx2/4* MO, *meis1*-morphant embryos, and *lzr*/*pbx4*$^{+/-}$ incross progeny injected with both *pbx2/4* MO and *meis1* MO. Consistent with the *in situ*

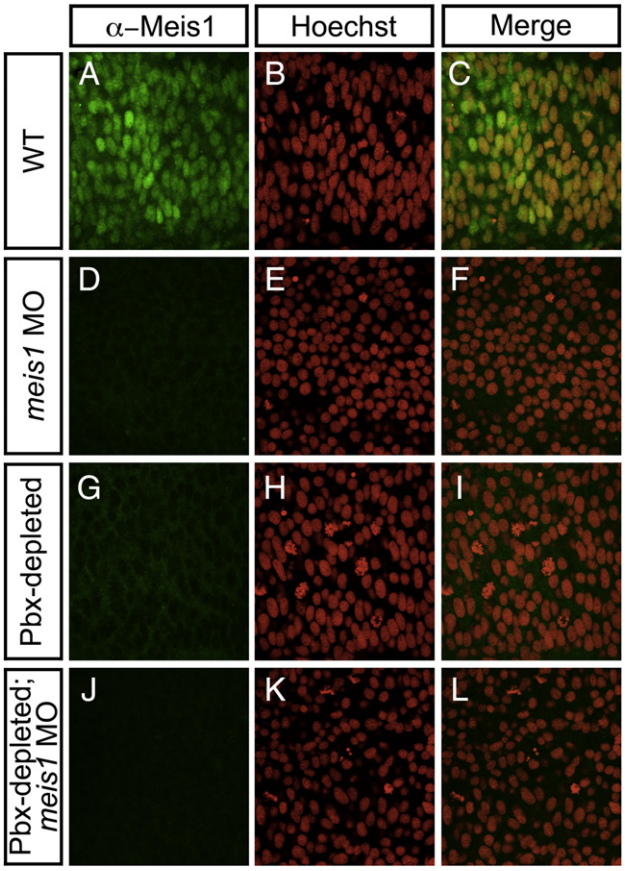

Fig. 3. Meis1 protein levels are severely diminished in the posterior mesoderm of Pbx-depleted and *meis1*-morphant embryos. Shown are representative embryos following immunohistochemical staining with the P2A6 antibody (green; A, D, G, J) to visualize Meis1 protein levels, and Hoechst 33258 (red; B, E, H, K) to visualize nuclei in 14 hpf wild type (WT; A–C), *meis1*-morphant (D–F), Pbx-depleted (G–I), and Pbx-depleted; *meis1*-morphant (J–L) embryos. Flat-mount; dorsal view of posterior mesoderm; anterior to left. All embryos visualized under a 100× objective. In wild type (WT; A–C) embryos, α-Meis1 antibody staining is punctate, and colocalizes with Hoechst nuclear staining. *meis1*-morphant (D) and Pbx-depleted (G) embryos exhibit severely decreased α-Meis1 antibody staining when compared to WT embryos (A). α-Meis1 antibody staining is further abolished in Pbx-depleted; *meis1*-morphant embryos (J). α-Meis1 antibody staining does not colocalize with Hoechst nuclear staining in Pbx-depleted embryos (G–I).

hybridization analysis, Pbx-depleted embryos exhibit a 28% decrease in *gata1* expression when compared to wild type embryos ($P<0.0001$, Fig. 4I). *meis1*-morphants exhibit a 26% decrease in *gata1* expression when compared to wild type embryos ($P<0.0001$, Fig. 4I). Embryos depleted of both Pbx and Meis1 exhibit a 50% decrease in *gata1* expression when compared to wild type embryos ($P<0.0001$, Fig. 4I). As one-quarter of the embryos injected with *pbx2/4* MO alone or in combination with *meis1* MO are on a *lzr/pbx4*$^{+/+}$ background, these embryos are not completely devoid of Pbx protein. Since embryo pools are collected at 16 hpf, a stage when phenotypic differences are not detectable, this quantitative PCR analysis likely under-represents the actual loss of *gata1* expression that occurs in both Pbx-depleted, and Pbx-depleted; *meis1*-morphant embryos.

Meis1 functions in association with Hox to regulate primitive erythropoiesis

Overexpressing *hoxb7a* or *hoxa9a* is sufficient to rescue *gata1* erythroid gene expression in embryos depleted of both Cdx1a and Cdx4 (Davidson and Zon, 2006), suggesting that these posteriorly-expressed *hox* genes act upstream of *gata1* to regulate erythropoiesis. Pbx and Meis proteins typically act as Hox protein cofactors (Moens and Selleri, 2006), and the posterior Hox proteins Hoxb7, Hoxa9, and Hoxd9 are able to form heterodimeric and heterotrimeric complexes with Pbx and Meis *in vitro* (Chang et al., 1997; Shanmugam et al., 1999). To determine if the posterior Hox proteins require Meis1 for their *in vivo* function, we injected *hoxb7a* mRNA into *meis1*-morphant embryos. As shown through *in situ* hybridization, overexpressing *hoxb7a* does not restore *gata1* erythroid gene expression in the PLM of 16 hpf *meis1*-morphant embryos (Figs. 5A–C). To measure *gata1* expression quantitatively, we performed real-time quantitative PCR

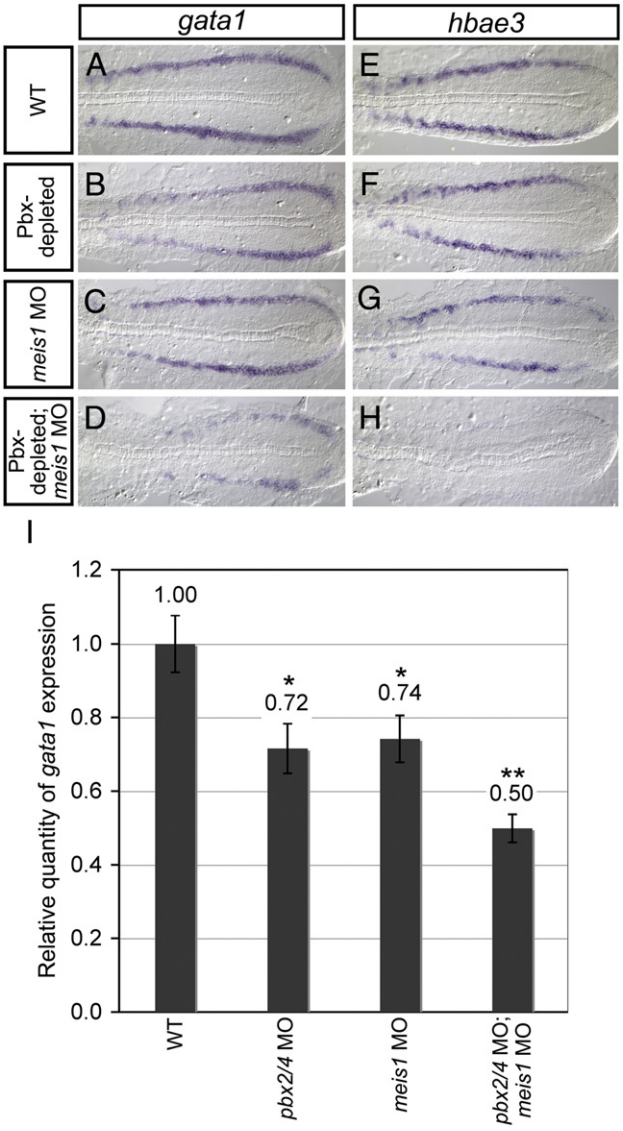

Fig. 4. Pbx and Meis1 act in a cooperative fashion to regulate erythroid gene expression. (A–H) Shown are representative embryos following *in situ* hybridization analysis of *gata1* (A–D) and *hbae3* (E–H) expression in 16 hpf embryos. Embryos shown are deyolked and flat-mounted with a dorsal view of gene expression in the PLM and anterior oriented to the left. Embryos partially depleted of Pbx (injected with 4.5 ng of *pbx2/4* MO) exhibit subtle decreases in *gata1* (B; 83%, $n=18$) and *hbae3* (F; 71%, $n=7$) expression. Embryos partially depleted of Meis1 (injected with 2 ng of *meis1* MO) exhibit subtle decreases in *gata1* (C; 85%, $n=20$) and *hbae3* (G; 100%, $n=6$) expression. Embryos partially depleted of both Pbx and Meis1 exhibit profoundly reduced *gata1* (D; 90%, $n=29$) and *hbae3* (H; 95%, $n=19$) expression. (I) Quantitative real-time PCR analysis of *gata1* expression in 16 hpf wild type embryos (WT), *lzr/pbx4*$^{+/-}$ incross progeny injected with a full dose of *pbx2/4* MO (*pbx2/4* MO), *meis1*-morphant embryos (*meis1* MO), and *lzr/pbx4*$^{+/-}$ incross progeny injected with a full dose of both *pbx2/4* MO and *meis1* MO (*pbx2/4* MO; *meis1* MO). Shown is the relative quantity of *gata1* expression. Samples were normalized to *ef1a* and WT was set to 1. Error bars indicate standard deviation from the mean. *Indicates the difference compared with WT is significant by Student *t* test, $P<0.0001$. **Indicates the difference compared with all other samples is significant by Student *t* test, $P<0.0001$.

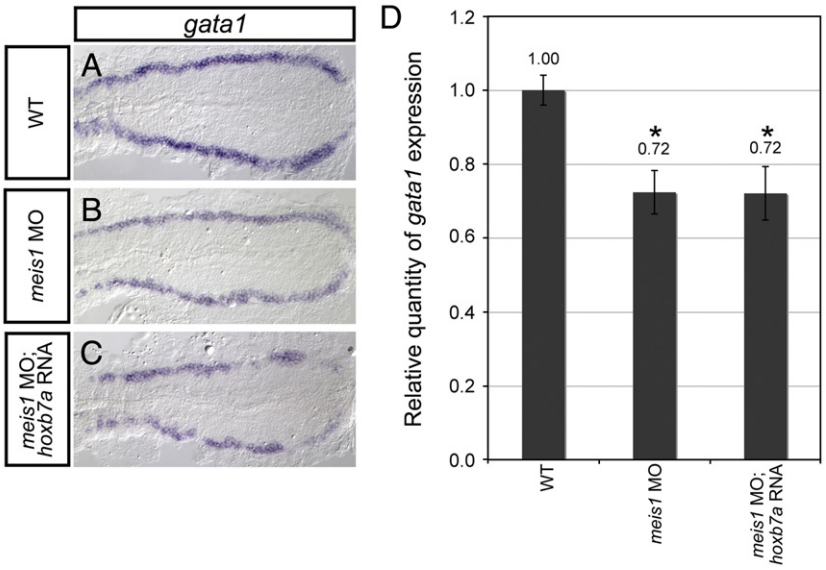

Fig. 5. Overexpressing *hoxb7a* rescues *gata1* erythroid gene expression in Pbx-depleted but not *meis1*-morphant embryos. (A–C) Shown are representative embryos following *in situ* hybridization analysis of *gata1* expression in 16 hpf embryos. Dorsal view of PLM gene expression is shown in flat-mounted and deyolked embryos, with anterior oriented to the left. Both *meis1*-morphant embryos (B; 94%, $n=63$) and *hoxb7a* RNA-injected *meis1*-morphant embryos (C; 91%, $n=43$) exhibit a severe decrease in *gata1* expression when compared to wild type embryos (WT; A). (D) Quantitative real-time PCR analysis of *gata1* expression in 16 hpf wild type embryos (WT), *meis1*-morphant embryos (*meis1* MO), and *hoxb7a* RNA-injected *meis1*-morphant embryos (*meis1* MO; *hoxb7a* RNA). Shown is the relative quantity of *gata1* expression. Samples were normalized to *ef1a* and WT was set to 1. Error bars indicate standard deviation from the mean. *Indicates the difference compared with WT is significant by Student *t* test; $P<0.0001$.

on 16 hpf wild type embryos, *meis1*-morphant embryos, and embryos injected with both *meis1* MO and *hoxb7a* mRNA. Consistent with the *in situ* hybridization analysis, both *meis1*-morphant embryos and *hoxb7a*-overexpressing *meis1*-morphant embryos exhibit a 28% decrease in *gata1* expression when compared to wild type embryos ($P<0.0001$ for each, Fig. 5D). Pbx-depleted and *meis1*-morphant embryos possess wild type levels of *hoxb6b*, *hoxb7a*, and *hoxa9a* gene expression at 16 hpf, as shown through *in situ* hybridization (Fig. S4). Western immunoblotting reveals that Hoxb7a protein stability is not dependent on the presence of Pbx or Meis1 (data not shown). Taken together, these data suggest that Hoxb7a requires Meis1 in order to activate *gata1* erythroid gene expression.

Meis1 and Pbx regulate primitive myelopoiesis

Overexpressing the zinc finger transcription factor GATA1 in myeloid cells inhibits myeloid differentiation, and induces a switch to megakaryocyte-erythroid cell fate (Iwasaki et al., 2003). Gata1-depleted zebrafish embryos display reduced numbers of erythrocytes, and expanded populations of granulocytic neutrophils and macrophages (Galloway et al., 2005; Rhodes et al., 2005), indicating that *gata1* represses myeloid differentiation, and is crucial for specifying erythroid cell fate. The molecular phenotype of Pbx-depleted and *meis1*-morphant embryos is similar to that of a Gata1-depleted embryo with regards to erythropoietic gene expression. Consequently, in order to determine if Pbx and Meis1 also serve to regulate myelopoiesis, we analyzed the expression of *pu.1* (*spi1*) in the anterior lateral-plate mesoderm (ALPM) of 24 hpf wild type, Pbx-depleted, and *meis1*-morphant embryos. *pu.1* is an Ets-family transcription factor that is responsible for specifying myeloid cell fate (Anderson et al., 1998; McKercher et al., 1996; Scott et al., 1994; Zhang et al., 1996). In comparison to their wild type counterparts (Figs. 6A, E), *meis1*-morphant embryos exhibit a significant 1.86-fold increase ($P<0.0001$) in the number of *pu.1*-expressing cells at 24 hpf, as shown through *in situ* hybridization analysis (Figs. 6B, E). Pbx-depleted embryos exhibit a significant 2.05-fold increase in the number of *pu.1*-expressing cells in comparison to wild type embryos ($P<0.0001$; Figs. 6A, C, E). Embryos depleted of both Pbx and Meis1 exhibit a more severe (2.60-fold) increase in the number of *pu.1*-positive cells than through removal of either protein alone ($P<0.0001$ for each when compared to wild type, Pbx-depleted, and *meis1*-morphant embryos; Figs. 6A–E). Consistent with our ALPM results, Pbx-depleted; *meis1*-morphant embryos also exhibit increased levels of ICM *pu.1* expression when compared to wild type embryos, as shown through *in situ* hybridization (Figs. 6F, G).

We next used *in situ* hybridization to analyze the expression *l-plastin* (*lcp1*) and *lysozyme C* (*lyz*) in the ALPM of 24 hpf wild type, Pbx-depleted, and *meis1*-morphant embryos. *lcp1* and *lyz* label macrophage and granulocyte progenitors (Hall et al., 2007; Le Guyader et al., 2008). In comparison to their wild type counterparts, both Pbx-depleted and *meis1*-morphant embryos exhibit an increase in the number of cells expressing *lcp1* (Figs. 6H–J) and *lyz* (Figs. 6K–M). Combined, these data suggest that Pbx and Meis1 act in a cooperative fashion to repress myeloid cell fate.

Pbx and Meis1 act upstream of gata1 to maintain proper levels of scl and hbae3, but not lmo2 expression

Our findings that Pbx-depleted and *meis1*-morphant embryos fail to initiate proper *gata1* expression, and possess similar defects in myelopoiesis to Gata1-depleted embryos imply that Pbx and Meis1 act upstream of *gata1* to regulate primitive hematopoiesis. To test this hypothesis, we first analyzed the maintenance of *scl* and *lmo2* in the ICM of 24 hpf *gata1*-morphant embryos. In comparison to their wild type counterparts, *gata1*-morphant embryos exhibit reduced *scl* expression at 24 hpf (Figs. 7C, D). These data suggest that, like Pbx and Meis1, Gata1 is required to maintain normal levels of *scl* expression at 24 hpf. Unlike Pbx-depleted (Fig. S2G') and *meis1*-morphant (Fig. 2G) embryos, *gata1*-morphant embryos exhibit wild type levels of *lmo2* expression at 24 hpf (Figs. 7A, B). Taken together, these data suggest that although Pbx and Meis1 are required to maintain normal levels of *lmo2* expression at 24 hpf, Gata1 is not.

In order to determine if the biological activity of *gata1* is dependent on the presence of Pbx and Meis1 protein, we first examined *scl* expression in the ICM of 24 hpf *gata1*-overexpressing *meis1*-morphant and Pbx-depleted embryos. As shown through *in situ* hybridization, *gata1*-overexpressing *meis1*-morphant (Fig. 7F) and Pbx-depleted (Fig. 7H) embryos display a greater level of *scl*

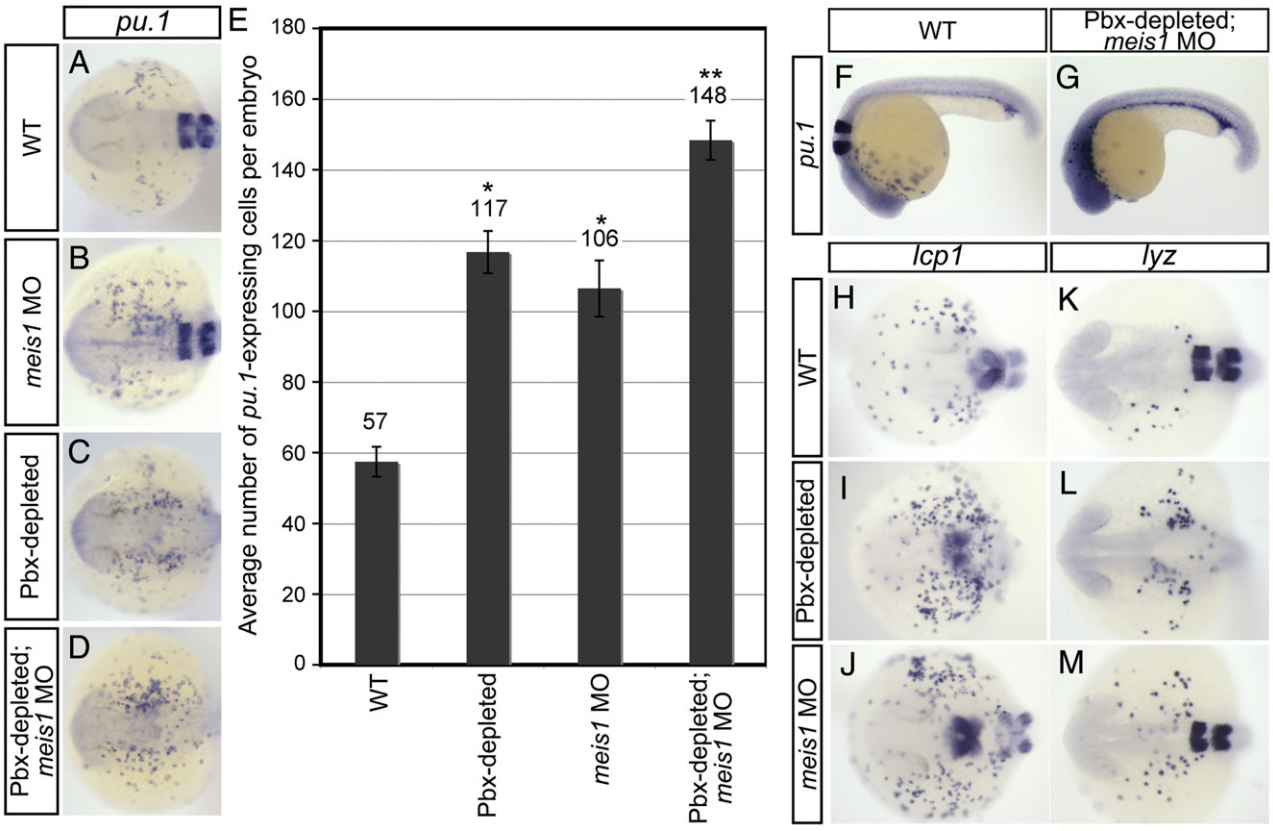

Fig. 6. Pbx and Meis1 act in a cooperative fashion to regulate primitive myelopoietic gene expression. (A–D) Shown are representative embryos following *in situ* hybridization analysis of *pu.1* expression in 24 hpf embryos. Dorsal view of gene expression in the anterior lateral-plate mesoderm (ALPM) is shown in whole-mount embryos with anterior oriented to the left. *meis1*-morphant (B), Pbx-depleted (C), and *meis1*-morphant; Pbx-depleted (D) embryos exhibit a severe increase in the number of *pu.1*-expressing cells when compared to wild type (WT; A) embryos. (E) Quantification of the phenotypes shown in A–D. Shown is the average number of *pu.1*-expressing cells in the ALPM of 24 hpf embryos as determined by *in situ* hybridization. Error bars indicate standard error of the mean. *Indicates the difference compared with WT is significant by Student *t* test; $P<0.0001$. **Indicates the difference compared to all other samples is significant by Student *t* test; $P<0.001$. (F–M) Shown are representative embryos following *in situ* hybridization analysis of *pu.1* (F, G) in lateral view, and *l-plastin* (*lcp1*; H–J) and *lysozyme C* (*lyz*; K–M) expression in dorsal view 24 hpf whole-mount embryos. Pbx-depleted; *meis1*-morphant embryos (G) exhibit upregulated *pu.1* expression in the intermediate cell mass when compared to WT embryos (F). Pbx-depleted (I, L), and *meis1*-morphant (J, M) embryos exhibit increased numbers of *lcp1* and *lyz*-positive cells in the ALPM when compared to WT embryos (H, K). Genotype of embryos was determined by *in situ* hybridization analysis of *egr2b* (F–M) and *eng2a* (H–J) expression.

expression than their *meis1*-morphant (Fig. 7E) and Pbx-depleted (Fig. 7G) counterparts, indicating that *gata1* is able to drive *scl* expression in the absence of Pbx and Meis1. We next examined *hbae3* expression in the PLM of 16 hpf *gata1*-overexpressing Pbx-depleted; *meis1*-morphant embryos. As shown through *in situ* hybridization, *gata1*-overexpression restores *hbae3* expression to near wild type levels in Pbx-depleted; *meis1*-morphant embryos (Figs. 7I–K), indicating that *gata1* is able to drive *hbae3* gene expression in the absence of Pbx and Meis1. Combined, these data suggest that Pbx and Meis1 act upstream of *gata1* to regulate the expression of *scl* and *hbae3*, but function independently of *gata1* to regulate *lmo2* expression.

Pbx-depleted; meis1-morphants and Cdx-depleted embryos exhibit distinct phenotypes

Previous research has shown that *cdx4*-mutant (*kgg*^{tv205}) embryos injected with Cdx1 morpholino (hereafter referred to as Cdx-depleted) are deficient for ICM blood precursors, and fail to properly initiate *scl* and *gata1* expression in the PLM at 12 hpf (Davidson and Zon, 2006). Cdx-depleted embryos also exhibit severe defects in *hoxb7a* and *hoxa9a* expression (Davidson and Zon, 2006). Furthermore, overexpressing these posteriorly-expressed *hox* genes partially rescues *gata1* expression in a Cdx-depleted embryo (Davidson and Zon, 2006). Taken together, these data suggest that *hox* genes act upstream of *gata1* to specify erythroid cell fate. Pbx and Meis proteins typically act as Hox protein cofactors (Moens and Selleri, 2006), and are essential for proper Hox function in the developing hindbrain (McNulty et al., 2005; Popperl et al., 2000; Vlachakis et al., 2001; Waskiewicz et al., 2002). We therefore wanted to determine if Cdx-depleted embryos and Pbx-depleted; *meis1*-morphant embryos exhibit comparable defects in erythropoietic gene expression. To do this, we examined the expression of *gata1* and *scl* in the PLM of wild type, Pbx-depleted; *meis1*-morphant, and Cdx-depleted embryos at 12 hpf, shortly after the initiation of *gata1* expression. As shown through *in situ* hybridization, *scl* is expressed at wild type levels in the PLM of 12 hpf Pbx-depleted; *meis1*-morphant embryos (Figs. 8A, B), but is abolished in the PLM of 12 hpf Cdx-depleted embryos (Figs. 8E, F). In contrast, *gata1* expression is abolished in Pbx-depleted; *meis1*-morphant (Figs. 8C, D) and Cdx-depleted (Figs. 8G, H) embryos at 12 hpf. *gata1* expression is also nearly abolished in Pbx-depleted embryos and *meis1*-morphants at 12 hpf (Fig. S5). To determine if the loss of *gata1* expression in Cdx-depleted embryos is attributable to a loss of Meis1, we examined *meis1* expression levels and Meis1 protein levels in 14 hpf Cdx-depleted embryos. Cdx-depleted embryos exhibit upregulated *meis1* expression and increased levels of anti-Meis1 antibody staining in comparison to wild type embryos (Fig. S3). Combined, these data suggest that Cdx functions independently of Meis1/Pbx to initiate the expression of *scl* and *gata1*.

Primitive erythropoietic gene expression is completely dependent on *scl* (Patterson et al., 2007; Shivdasani et al., 1995). It is therefore plausible that the erythropoietic defects of Cdx-depleted embryos (i.e.

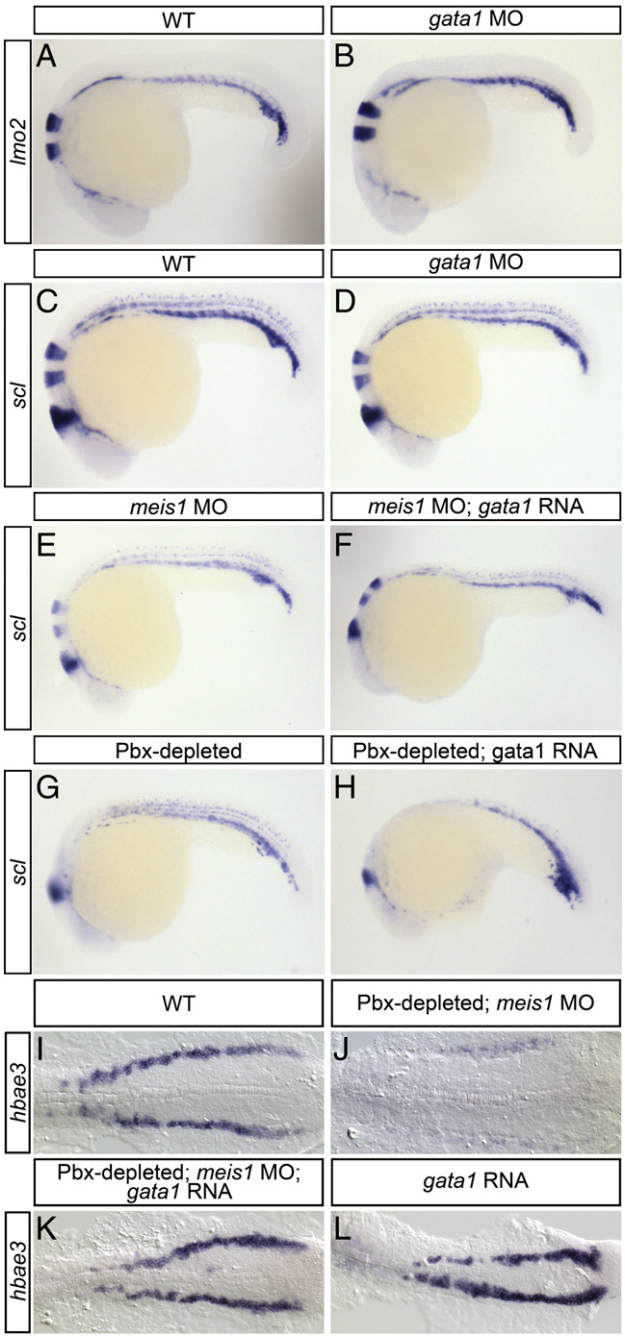

Fig. 7. Pbx and Meis1 act upstream of *gata1* to regulate the expression of *hbae3* and *scl*, but not *lmo2*. (A–H) Shown are representative embryos following *in situ* hybridization analyses of *lmo2* and *scl* expression in lateral view 24 hpf whole-mount embryos. *gata1*-morphant embryos (B; 100%, $n=11$) exhibit near normal *lmo2* expression when compared to WT embryos (A). *gata1*-morphant (D; 100%, $n=7$), *meis1*-morphant (E; 100%, $n=6$), and Pbx-depleted (G; 94%, $n=16$) embryos exhibit diminished *scl* expression in the ICM when compared to wild type (WT; C) embryos. *meis1*-morphant, *gata1* RNA-injected embryos (F; 100%, $n=5$), and Pbx-depleted, *gata1* RNA-injected embryos (H; 95%, $n=19$) exhibit greater levels of *scl* expression than respective *meis1*-morphant (E) and Pbx-depleted (G) counterparts. Genotype of embryos was determined by *in situ* hybridization analysis of *egr2b* expression in hindbrain rhombomeres 3 and 5 (A–H), and *eng2a* expression in the midbrain hindbrain boundary and muscle pioneers (C–H). (I–L) Shown are representative embryos following *in situ* hybridization analysis of *hbae3* expression in 16 hpf embryos. Dorsal view of PLM gene expression is shown in deyolked, flat-mounted embryos with anterior oriented to the left. Pbx-depleted; *meis1*-morphant embryos (J; 90%, $n=10$) exhibit nearly abolished *hbae3* expression when compared to WT embryos (I). *gata1* RNA-injected, Pbx-depleted; *meis1*-morphant embryos (K; 82%, $n=11$) exhibit near normal *hbae3* expression. *gata1* RNA-injected embryos (L; 100%, $n=4$) exhibit slightly increased *hbae3* expression when compared to WT embryos (I).

loss of *gata1* and *hbae3*) represent indirect results of abolished *scl* expression. Overexpressing *hoxb7a* generates an increase in *gata1* expression (data not shown), and can partially rescue *gata1* expression in a Cdx-depleted embryo (Fig. S6; Davidson and Zon, 2006). *hoxb7a* overexpression fails to rescue *gata1* expression in *meis1*-morphant embryos (Fig. 5C), or Pbx-depleted; *meis1*-morphant embryos (Fig. S6), suggesting that Hox function depends on the presence of Meis1 protein. Taken together, these results are consistent with a model that places *hox* and its cofactor *meis1* on a parallel pathway to *scl*, and upstream of *gata1* (Fig. 8I).

Discussion

Previous research has shown that the TALE-class homeodomain transcription factors Meis and Pbx function as critical regulators of definitive hematopoiesis (Azcoitia et al., 2005; Di Rosa et al., 2007; DiMartino et al., 2001; Ferretti et al., 2006; Hisa et al., 2004). Our study describes a novel role for Meis1 and Pbx in primitive hematopoiesis. We propose that Meis1 and Pbx function near the top of a hierarchy of transcription factors that regulate the development of primitive erythrocytes (Fig. 8I). Through targeted ablation of Meis1 and Pbx proteins, we demonstrate that Meis1 and Pbx are required for the transcriptional activation of *gata1*, a gene that has an evolutionarily conserved role in specifying erythroid cell fate (Galloway et al., 2005; Pevny et al., 1991; Rhodes et al., 2005; Shivdasani et al., 1997). Consequently, in the absence of Meis1 and Pbx, embryos exhibit severe defects in primitive erythropoiesis, and are unable to produce visible circulating blood cells. Concomitant with a loss of *gata1*, Meis1 and Pbx-depleted embryos also exhibit increased numbers of myelocytes, and fail to maintain wild type levels of *scl*, a broad marker of hematopoietic cell fate.

Meis1 and Pbx in the erythropoietic transcription factor hierarchy

Inhibiting Meis1 and Pbx function reduces the expression of genes that specify primitive erythrocyte identity. *meis1*-morphant and Pbx-depleted embryos fail to properly initiate *gata1*, a transcription factor that is essential for erythrocyte development (Galloway et al., 2005; Lyons et al., 2002; Pevny et al., 1991; Rhodes et al., 2005; Shivdasani et al., 1997). These embryos also exhibit downregulated expression of the embryonic hemoglobin gene *hbae3*, which is a downstream target of *gata1* (data not shown). The expression of *scl*, a broad marker of hematopoietic cell fate, is initiated normally, but not maintained at wild type levels in embryos lacking Meis1 and Pbx. Gata transcription factors act as part of multiprotein complexes that bind the autoregulatory enhancer of *scl* (Gottgens et al., 2002; Orkin, 1992). We demonstrate that *gata1*-morphant embryos likewise fail to maintain normal levels of *scl* expression, and this molecular phenotype is also observed in *gata1*-mutant (vlt^{m651}) embryos (Lyons et al., 2002). We also demonstrate that *gata1* overexpression is able to drive *scl* and *hbae3* expression in *meis1*-morphant and Pbx-depleted embryos. Taken together, these data support a model in which Meis1 and Pbx regulate erythropoiesis by activating *gata1*, which is subsequently required to activate *hbae3* and maintain wild type levels of *scl* expression in maturing erythrocytes (Fig. 8I).

Although *lmo2* is a broad marker of hematopoietic cell fate, previous research has highlighted its importance in specifying the erythroid lineage. For example, *Lmo2*-mutant mice possess severe embryonic-lethal defects in erythropoiesis (Warren et al., 1994). Like with *scl*, the expression of *lmo2* is initiated normally, but not maintained at wild type levels in *meis1*-morphant and Pbx-depleted embryos. However, we demonstrate that *lmo2* expression, unlike *scl* expression, is maintained normally in Gata1-depleted embryos. These data suggest that Meis1 and Pbx act in a *gata1*-independent fashion to regulate the expression of *lmo2*. The transcriptional regulation of *scl* and *lmo2* is also uncoupled in *cloche* (clo^{m39}) mutant zebrafish

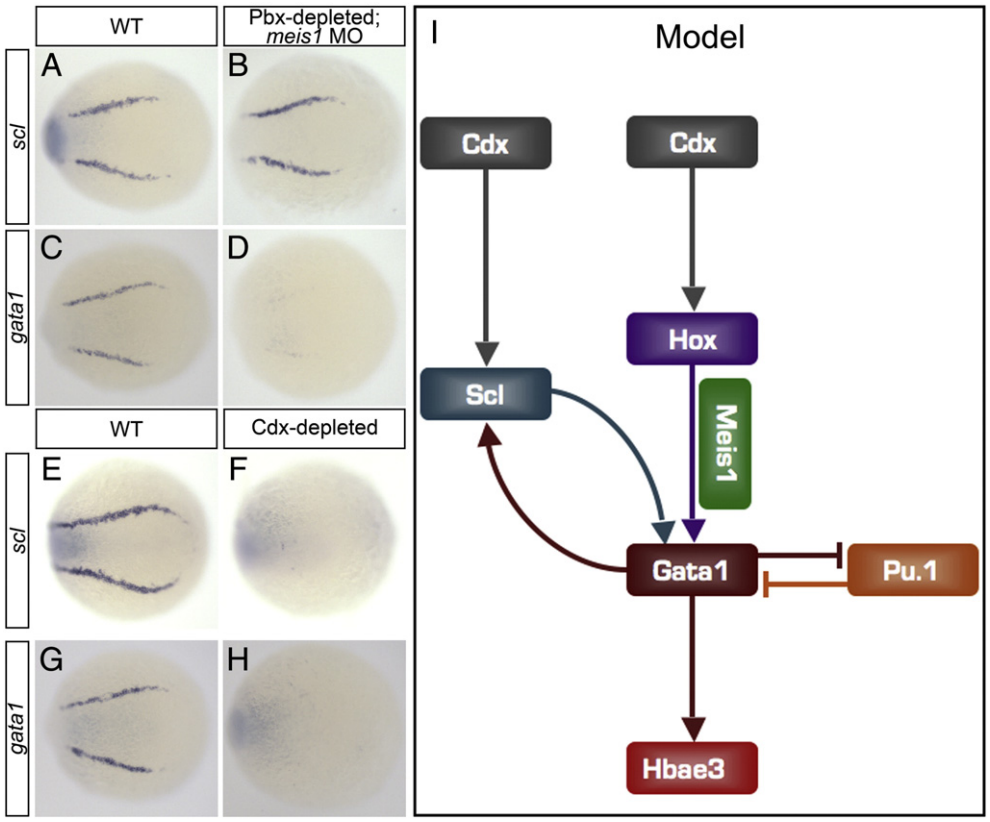

Fig. 8. Unlike Cdx, Meis1 and Pbx function downstream of *scl* to activate *gata1* expression. (A–H) Shown are representative embryos following *in situ* hybridization analysis of *scl* and *gata1* expression in 12 hpf embryos. Dorsal view of gene expression in the posterior lateral-plate mesoderm (PLM) is shown in whole-mount embryos with anterior oriented to the left. Pbx-depleted; *meis1*-morphant embryos exhibit wild type (WT) levels of *scl* expression (B; 100%, $n=13$) and abolished *gata1* expression (D; 100%, $n=18$) when compared to WT (A, C) embryos. Genotype of Pbx-depleted; *meis1*-morphant embryos was determined by *in situ* hybridization analysis of *egr2b* expression. Cdx-depleted embryos exhibit abolished *scl* (F; 100%, $n=5$) and *gata1* (H; 100%, $n=7$) expression when compared to WT (E, G) embryos. (I) Hierarchical model indicating the genetic interactions that occur between a subset of transcription factors that regulate zebrafish primitive hematopoiesis. Arrows do not necessarily represent direct interactions.

(Dooley et al., 2005). Consequently, our study identifies Meis1 and Pbx as novel targets for elucidating the mechanisms by which *lmo2* and *scl* are independently regulated.

Pbx and Meis1 in primitive myelopoiesis

The interplay between *gata1* and *pu.1* in specifying erythroid versus myeloid cell fate is well characterized. Biochemical evidence suggests that GATA1 and PU.1 proteins physically interact to inhibit the transcriptional regulation of each other's target genes (Nerlov et al., 2000; Rekhtman et al., 1999; Stopka et al., 2005; Zhang et al., 1999, 2000). Furthermore, Pu.1-depleted zebrafish embryos exhibit ectopic *gata1* expression in the anterior lateral-plate mesoderm (ALPM) (Rhodes et al., 2005), suggesting that Pu.1 transcriptionally represses *gata1*. In a reciprocal fashion, Gata1-depleted zebrafish embryos demonstrate increased numbers of *pu.1*-positive cells in the intermediate cell mass (ICM) and ALPM (Galloway et al., 2005; Lyons et al., 2002; Rhodes et al., 2005). As previously mentioned, *meis1*-morphant and Pbx-depleted embryos exhibit diminished *gata1* expression. In key with these findings, these embryos also exhibit increased numbers of *pu.1*-positive ALPM and ICM cells. Consequently, because *meis1*-morphant and Pbx-depleted embryos phenocopy Gata1-depleted embryos with regards to both erythropoietic and myelopoietic gene expression defects, we can place *meis1* upstream of *gata1* in the primitive myelopoietic transcription factor hierarchy. Furthermore, given that *pu.1* expression is upregulated in the ICM of Pbx-depleted; *meis1*-morphant embryos, we postulate that the loss of *gata1* expression in these embryos represents a switch from erythroid to myeloid cell fate.

Distinct requirements for Pbx and Meis1 in primitive hematopoiesis

Pbx and Meis/Prep1 proteins associate with each other through conserved motifs situated N-terminal to their respective homeodomains (Berthelsen et al., 1998b; Knoepfler et al., 1997). This interaction occurs even in the absence of DNA (Knoepfler et al., 1997). Previous research has demonstrated a role for Meis/Prep1 in stabilizing Pbx, and regulating its nuclear import (Abu-Shaar et al., 1999; Berthelsen et al., 1999; Mercader et al., 1999; Stevens and Mann, 2007; Waskiewicz et al., 2001). In a reciprocal fashion, recent work in *Drosophila* has demonstrated that Hth (Homothorax; orthologue of Meis) requires Exd (Extrandenticle; orthologue of Pbx) to achieve nuclear import and stability (Stevens and Mann, 2007). In zebrafish, we similarly demonstrate that Pbx stabilizes Meis1, and is required for its nuclear import *in vivo*. Pbx-depleted zebrafish exhibit wild type levels of *meis1* expression at 12 hpf, and downregulated *meis1* expression at 24 hpf, as shown through *in situ* hybridization analyses (T. Erickson, unpublished). Taken together, these data suggest that Pbx acts in a pre- and post-transcriptional fashion to regulate Meis1 protein levels.

Other Meis-family proteins, such as Prep1, are present in the developing embryo during primitive hematopoiesis. Furthermore, previous research has demonstrated the capacity of Pbx to be nuclear-localized in the absence of Meis/Prep1 (Kilstrup-Nielsen et al., 2003). It is therefore unlikely that Pbx is dependent solely on Meis1 for its stabilization and nuclear import. For these reasons, we hypothesize that the hematopoietic defects we observe in *meis1*-morphant and Pbx-depleted embryos are due to a specific transcriptional requirement for Meis1. Our immunohistochemical data suggests that *meis1*-morphant embryos mimic hypomorphs, providing an explanation for

why Pbx-depleted; *meis1*-morphant embryos exhibit more severe defects in *gata1* and *hbae3* expression than Pbx-depleted or *meis1*-morphant embryos.

Pbx and Meis1 as Hox cofactors in primitive hematopoiesis

Pbx and Meis proteins form heterodimeric and heterotrimeric complexes with Hox proteins (Berthelsen et al., 1998a; Chang et al., 1995, 1996; Ferretti et al., 2000; Jacobs et al., 1999; Mann and Chan, 1996; Ryoo et al., 1999; Sarno et al., 2005; Shanmugam et al., 1999; Shen et al., 1997a,b, 1999; Vlachakis et al., 2001; Williams et al., 2005). These interactions are necessary for proper anteroposterior patterning of the developing hindbrain (Cooper et al., 2003; Vlachakis et al., 2001; Waskiewicz et al., 2001, 2002). In zebrafish, the posteriorly-expressed *hox* genes *hoxb6b*, *hoxb7a*, and *hoxa9a* have been implicated in the transcriptional regulation of primitive erythropoietic genes such as *gata1* (Davidson et al., 2003; Davidson and Zon, 2006). Biochemical analyses have demonstrated the capacity of Pbx and Meis proteins to bind posterior Hox proteins *in vitro* (Chang et al., 1995, 1996; Mann and Chan, 1996; Sarno et al., 2005; Shanmugam et al., 1999; Shen et al., 1997a,b, 1999; Williams et al., 2005). We demonstrate that overexpressing *hoxb7a* fails to rescue the *gata1* erythroid gene expression defects of *meis1*-morphant embryos. Given that *meis1*-morphant embryos exhibit wild type levels of *hoxb7a* expression and normal levels of overexpressed Hoxb7a protein, these data suggest that Hoxb7a specifically requires Meis1 protein in order to transcriptionally regulate *gata1*.

Implications for Hox function in primitive hematopoiesis

The role of Hox function in hematopoiesis has been studied extensively in mice with targeted deletions in *Hoxb3*, *Hoxb4*, *Hoxb6*, *Hoxa7*, *Hoxc8*, and *Hoxa9* respectively (Bjornsson et al., 2003; Brun et al., 2004; Izon et al., 1998; Kappen, 2000; Ko et al., 2007; Lawrence et al., 1997; Magnusson et al., 2007a; Shimamoto et al., 1999; So et al., 2004). Mice with mutations in *Hoxa9*, *Hoxb4*, or *Hoxb3* exhibit similar defects in the capacity of hematopoietic stem cells to repopulate (Bjornsson et al., 2003; Brun et al., 2004; Lawrence et al., 1997). The hematopoietic defects observed in mice with compound mutations in *Hoxb3*, *Hoxb4* and *Hoxa9* are more severe than those observed in *Hoxa9*-mutant mice (Magnusson et al., 2007a), suggesting that Hox transcription factors perform overlapping functions in hematopoiesis. A more global analysis of Hox function in primitive hematopoiesis is achieved through knockdown of the homeodomain transcription factor Cdx. Previous research has shown that *cdx4*-mutant (*kgg*^{tv205}) zebrafish exhibit decreased expression of the posteriorly-expressed *hox* genes *hoxb6b*, *hoxb7a*, *hoxb8b*, and *hoxa9a* (Davidson et al., 2003). Notably, the expression of many *hox* genes is normal in Cdx-depleted embryos, and the expression of some posteriorly-expressed *hox* genes, such as *hoxb5b*, is markedly expanded (Davidson et al., 2003; Davidson and Zon, 2006). These embryos also possess severe defects in primitive erythropoiesis (Davidson et al., 2003; Davidson and Zon, 2006) that are in some ways similar to those observed in *meis1*-morphant and Pbx-depleted embryos. For example, Cdx-depleted embryos fail to initiate *gata1* erythroid gene expression, but exhibit normal rostral angioblast expression of *flk1a* (Davidson and Zon, 2006). Cdx-depleted embryos are also strikingly different from *meis1*-morphant and Pbx-depleted embryos. The posterior *hox* genes *hoxb6b*, *hoxb7a*, and *hoxa9a* are expressed at normal levels in *meis1*-morphant and Pbx-depleted embryos. Furthermore, whereas Cdx-depleted embryos exhibit defects in the initiation of *scl* expression (Davidson and Zon, 2006), *scl* expression is initiated normally, but not maintained at proper levels in embryos lacking Meis1 and Pbx. *scl* overexpression generates increased populations of *gata1*-expressing cells in a Cdx4-dependent manner (Davidson et al., 2003). Conversely, *hox* overexpression drives *gata1* expression in the absence of Cdx4 (Fig. S6; Davidson et al., 2003; Davidson and Zon, 2006). Taken together with our own data, these data place Hox upstream of *gata1* in the primitive hematopoietic transcription factor hierarchy. These data also suggest that Cdx acts in a *hox*-independent fashion to initiate *scl* expression. We therefore propose a model whereby Cdx activates Hox, which together with Meis1 activates *gata1* erythroid gene expression (Fig. 8I). Previous research has shown that Hoxa10 has the capacity to bind directly to the *gata1* promoter (Magnusson et al., 2007b). Meis1 and Pbx form heterotrimeric complexes with posterior Hox proteins including Hoxa10 (Shanmugam et al., 1999). Consequently, the transcriptional activation of *gata1* by Pbx and Meis1 may occur in a direct fashion.

Acknowledgments

We thank members of the Waskiewicz Laboratory for technical assistance and constructive comments. We also thank Aleah McCorry, Erin Pemberton, and Robyn Shortt for fish care, as well as Honey Chan, Andrew Simmonds, and Rakesh Bhatnagar for help with confocal microscopy.

This work was supported by CIHR (A.J.W.) and a CIHR-NSHRF regional partnership grant (J.N.B.). Salary support was provided by Alberta Ingenuity Fund (L.M.P., T.E.), NSERC (L.M.P, T.E.), CIHR (A.M.F.), Canadian Cancer Society (A.M.F.), and a Dalhousie University Clinical Scholar Award (J.N.B.). A.J.W. is a Canada Research Chair.

Appendix A. Supplementary data

Supplementary data associated with this article can be found, in the online version, at doi:10.1016/j.ydbio.2010.01.033.

References

Abramovich, C., Humphries, R.K., 2005. Hox regulation of normal and leukemic hematopoietic stem cells. Curr. Opin. Hematol. 12, 210–216.

Abu-Shaar, M., Ryoo, H.D., Mann, R.S., 1999. Control of the nuclear localization of Extradenticle by competing nuclear import and export signals. Genes Dev. 13, 935–945.

Anderson, K.L., Smith, K.A., Conners, K., McKercher, S.R., Maki, R.A., Torbett, B.E., 1998. Myeloid development is selectively disrupted in PU.1 null mice. Blood 91, 3702–3710.

Azcoitia, V., Aracil, M., Martinez, A.C., Torres, M., 2005. The homeodomain protein Meis1 is essential for definitive hematopoiesis and vascular patterning in the mouse embryo. Dev. Biol. 280, 307–320.

Baumann, R., Dragon, S., 2005. Erythropoiesis and red cell function in vertebrate embryos. Eur. J. Clin. Invest. 35 (Suppl 3), 2–12.

Berthelsen, J., Zappavigna, V., Ferretti, E., Mavilio, F., Blasi, F., 1998a. The novel homeoprotein Prep1 modulates Pbx–Hox protein cooperativity. EMBO J. 17, 1434–1445.

Berthelsen, J., Zappavigna, V., Mavilio, F., Blasi, F., 1998b. Prep1, a novel functional partner of Pbx proteins. EMBO J. 17, 1423–1433.

Berthelsen, J., Kilstrup-Nielsen, C., Blasi, F., Mavilio, F., Zappavigna, V., 1999. The subcellular localization of PBX1 and EXD proteins depends on nuclear import and export signals and is modulated by association with PREP1 and HTH. Genes Dev. 13, 946–953.

Bjornsson, J.M., Larsson, N., Brun, A.C., Magnusson, M., Andersson, E., Lundstrom, P., Larsson, J., Repetowska, E., Ehinger, M., Humphries, R.K., Karlsson, S., 2003. Reduced proliferative capacity of hematopoietic stem cells deficient in Hoxb3 and Hoxb4. Mol. Cell. Biol. 23, 3872–3883.

Brun, A.C., Bjornsson, J.M., Magnusson, M., Larsson, N., Leveen, P., Ehinger, M., Nilsson, E., Karlsson, S., 2004. Hoxb4-deficient mice undergo normal hematopoietic development but exhibit a mild proliferation defect in hematopoietic stem cells. Blood 103, 4126–4133.

Chan, S.K., Mann, R.S., 1996. A structural model for a homeotic protein–extradenticle–DNA complex accounts for the choice of HOX protein in the heterodimer. Proc. Natl. Acad. Sci. U. S. A. 93, 5223–5228.

Chan, S.K., Popperl, H., Krumlauf, R., Mann, R.S., 1996. An extradenticle-induced conformational change in a HOX protein overcomes an inhibitory function of the conserved hexapeptide motif. EMBO J. 15, 2476–2487.

Chang, C.P., Shen, W.F., Rozenfeld, S., Lawrence, H.J., Largman, C., Cleary, M.L., 1995. Pbx proteins display hexapeptide-dependent cooperative DNA binding with a subset of Hox proteins. Genes Dev. 9, 663–674.

Chang, C.P., Brocchieri, L., Shen, W.F., Largman, C., Cleary, M.L., 1996. Pbx modulation of Hox homeodomain amino-terminal arms establishes different DNA-binding specificities across the Hox locus. Mol. Cell. Biol. 16, 1734–1745.

Chang, C.P., Jacobs, Y., Nakamura, T., Jenkins, N.A., Copeland, N.G., Cleary, M.L., 1997. Meis proteins are major in vivo DNA binding partners for wild-type but not chimeric Pbx proteins. Mol. Cell. Biol. 17, 5679–5687.
Cooper, K.L., Leisenring, W.M., Moens, C.B., 2003. Autonomous and nonautonomous functions for Hox/Pbx in branchiomotor neuron development. Dev. Biol. 253, 200–213.
Davidson, A.J., Zon, L.I., 2006. The caudal-related homeobox genes cdx1a and cdx4 act redundantly to regulate hox gene expression and the formation of putative hematopoietic stem cells during zebrafish embryogenesis. Dev. Biol. 292, 506–518.
Davidson, A.J., Ernst, P., Wang, Y., Dekens, M.P., Kingsley, P.D., Palis, J., Korsmeyer, S.J., Daley, G.Q., Zon, L.I., 2003. cdx4 mutants fail to specify blood progenitors and can be rescued by multiple hox genes. Nature 425, 300–306.
Di Rosa, P., Villaescusa, J.C., Longobardi, E., Iotti, G., Ferretti, E., Diaz, V.M., Miccio, A., Ferrari, G., Blasi, F., 2007. The homeodomain transcription factor Prep1 (pKnox1) is required for hematopoietic stem and progenitor cell activity. Dev. Biol. 311, 324–334.
DiMartino, J.F., Selleri, L., Traver, D., Firpo, M.T., Rhee, J., Warnke, R., O'Gorman, S., Weissman, I.L., Cleary, M.L., 2001. The Hox cofactor and proto-oncogene Pbx1 is required for maintenance of definitive hematopoiesis in the fetal liver. Blood 98, 618–626.
Dooley, K.A., Davidson, A.J., Zon, L.I., 2005. Zebrafish scl functions independently in hematopoietic and endothelial development. Dev. Biol. 277, 522–536.
Ebner, A., Cabernard, C., Affolter, M., Merabet, S., 2005. Recognition of distinct target sites by a unique Labial/Extradenticle/Homothorax complex. Development 132, 1591–1600.
Erickson, T., Scholpp, S., Brand, M., Moens, C.B., Waskiewicz, A.J., 2007. Pbx proteins cooperate with Engrailed to pattern the midbrain–hindbrain and diencephalic–mesencephalic boundaries. Dev. Biol. 301, 504–517.
Ferretti, E., Marshall, H., Popperl, H., Maconochie, M., Krumlauf, R., Blasi, F., 2000. Segmental expression of Hoxb2 in r4 requires two separate sites that integrate cooperative interactions between Prep1, Pbx and Hox proteins. Development 127, 155–166.
Ferretti, E., Villaescusa, J.C., Di Rosa, P., Fernandez-Diaz, L.C., Longobardi, E., Mazzieri, R., Miccio, A., Micali, N., Selleri, L., Ferrari, G., Blasi, F., 2006. Hypomorphic mutation of the TALE gene Prep1 (pKnox1) causes a major reduction of Pbx and Meis proteins and a pleiotropic embryonic phenotype. Mol. Cell. Biol. 26, 5650–5662.
French, C.R., Erickson, T., Callander, D., Berry, K.M., Koss, R., Hagey, D.W., Stout, J., Wuennenberg-Stapleton, K., Ngai, J., Moens, C.B., Waskiewicz, A.J., 2007. Pbx homeodomain proteins pattern both the zebrafish retina and tectum. BMC Dev. Biol. 7, 85.
French, C.R., Erickson, T., French, D.V., Pilgrim, D.B., Waskiewicz, A.J., 2009. Gdf6a is required for the initiation of dorsal–ventral retinal patterning and lens development. Dev. Biol. 333, 37–47.
Galloway, J.L., Wingert, R.A., Thisse, C., Thisse, B., Zon, L.I., 2005. Loss of gata1 but not gata2 converts erythropoiesis to myelopoiesis in zebrafish embryos. Dev. Cell 8, 109–116.
Gering, M., Rodaway, A.R., Gottgens, B., Patient, R.K., Green, A.R., 1998. The SCL gene specifies haemangioblast development from early mesoderm. EMBO J. 17, 4029–4045.
Gering, M., Yamada, Y., Rabbitts, T.H., Patient, R.K., 2003. Lmo2 and Scl/Tal1 convert non-axial mesoderm into haemangioblasts which differentiate into endothelial cells in the absence of Gata1. Development 130, 6187–6199.
Gongal, P.A., Waskiewicz, A.J., 2008. Zebrafish model of holoprosencephaly demonstrates a key role for TGIF in regulating retinoic acid metabolism. Hum. Mol. Genet. 17, 525–538.
Gottgens, B., Nastos, A., Kinston, S., Piltz, S., Delabesse, E.C., Stanley, M., Sanchez, M.J., Ciau-Uitz, A., Patient, R., Green, A.R., 2002. Establishing the transcriptional programme for blood: the SCL stem cell enhancer is regulated by a multiprotein complex containing Ets and GATA factors. EMBO J. 21, 3039–3050.
Hall, C., Flores, M.V., Storm, T., Crosier, K., Crosier, P., 2007. The zebrafish lysozyme C promoter drives myeloid-specific expression in transgenic fish. BMC Dev. Biol. 7, 42.
Hisa, T., Spence, S.E., Rachel, R.A., Fujita, M., Nakamura, T., Ward, J.M., Devor-Henneman, D.E., Saiki, Y., Kutsuna, H., Tessarollo, L., Jenkins, N.A., Copeland, N.G., 2004. Hematopoietic, angiogenic and eye defects in Meis1 mutant animals. EMBO J. 23, 450–459.
Hove, J.R., Koster, R.W., Forouhar, A.S., Acevedo-Bolton, G., Fraser, S.E., Gharib, M., 2003. Intracardiac fluid forces are an essential epigenetic factor for embryonic cardiogenesis. Nature 421, 172–177.
Iwasaki, H., Mizuno, S., Wells, R.A., Cantor, A.B., Watanabe, S., Akashi, K., 2003. GATA-1 converts lymphoid and myelomonocytic progenitors into the megakaryocyte/erythrocyte lineages. Immunity 19, 451–462.
Izon, D.J., Rozenfeld, S., Fong, S.T., Komuves, L., Largman, C., Lawrence, H.J., 1998. Loss of function of the homeobox gene Hoxa-9 perturbs early T-cell development and induces apoptosis in primitive thymocytes. Blood 92, 383–393.
Jacobs, Y., Schnabel, C.A., Cleary, M.L., 1999. Trimeric association of Hox and TALE homeodomain proteins mediates Hoxb2 hindbrain enhancer activity. Mol. Cell. Biol. 19, 5134–5142.
Jaw, T.J., You, L.R., Knoepfler, P.S., Yao, L.C., Pai, C.Y., Tang, C.Y., Chang, L.P., Berthelsen, J., Blasi, F., Kamps, M.P., Sun, Y.H., 2000. Direct interaction of two homeoproteins, homothorax and extradenticle, is essential for EXD nuclear localization and function. Mech. Dev. 91, 279–291.
Kappen, C., 2000. Disruption of the homeobox gene Hoxb-6 in mice results in increased numbers of early erythrocyte progenitors. Am. J. Hematol. 65, 111–118.
Kilstrup-Nielsen, C., Alessio, M., Zappavigna, V., 2003. PBX1 nuclear export is regulated independently of PBX–MEINOX interaction by PKA phosphorylation of the PBC-B domain. EMBO J. 22, 89–99.
Kimmel, C.B., Ballard, W.W., Kimmel, S.R., Ullmann, B., Schilling, T.F., 1995. Stages of embryonic development of the zebrafish. Dev. Dyn. 203, 253–310.
Knoepfler, P.S., Lu, Q., Kamps, M.P., 1996. Pbx-1 Hox heterodimers bind DNA on inseparable half-sites that permit intrinsic DNA binding specificity of the Hox partner at nucleotides 3′ to a TAAT motif. Nucleic Acids Res. 24, 2288–2294.
Knoepfler, P.S., Calvo, K.R., Chen, H., Antonarakis, S.E., Kamps, M.P., 1997. Meis1 and pKnox1 bind DNA cooperatively with Pbx1 utilizing an interaction surface disrupted in oncoprotein E2a-Pbx1. Proc. Natl. Acad. Sci. U. S. A. 94, 14553–14558.
Ko, K.H., Lam, Q.L., Zhang, M., Wong, C.K., Lo, C.K., Kahmeyer-Gabbe, M., Tsang, W.H., Tsang, S.L., Chan, L.C., Sham, M.H., Lu, L., 2007. Hoxb3 deficiency impairs B lymphopoiesis in mouse bone marrow. Exp. Hematol. 35, 465–475.
Kroon, E., Thorsteinsdottir, U., Mayotte, N., Nakamura, T., Sauvageau, G., 2001. NUP98-HOXA9 expression in hemopoietic stem cells induces chronic and acute myeloid leukemias in mice. EMBO J. 20, 350–361.
LaRonde-LeBlanc, N.A., Wolberger, C., 2003. Structure of HoxA9 and Pbx1 bound to DNA: Hox hexapeptide and DNA recognition anterior to posterior. Genes Dev. 17, 2060–2072.
Lawrence, H.J., Helgason, C.D., Sauvageau, G., Fong, S., Izon, D.J., Humphries, R.K., Largman, C., 1997. Mice bearing a targeted interruption of the homeobox gene HOXA9 have defects in myeloid, erythroid, and lymphoid hematopoiesis. Blood 89, 1922–1930.
Le Guyader, D., Redd, M.J., Colucci-Guyon, E., Murayama, E., Kissa, K., Briolat, V., Mordelet, E., Zapata, A., Shinomiya, H., Herbomel, P., 2008. Origins and unconventional behavior of neutrophils in developing zebrafish. Blood 111, 132–141.
Lieschke, G.J., Oates, A.C., Crowhurst, M.O., Ward, A.C., Layton, J.E., 2001. Morphologic and functional characterization of granulocytes and macrophages in embryonic and adult zebrafish. Blood 98, 3087–3096.
Livak, K.J., Schmittgen, T.D., 2001. Analysis of relative gene expression data using real-time quantitative PCR and the 2(−Delta Delta C(T)) Method. Methods 25, 402–408.
Longobardi, E., Blasi, F., 2003. Overexpression of PREP-1 in F9 teratocarcinoma cells leads to a functionally relevant increase of PBX-2 by preventing its degradation. J. Biol. Chem. 278, 39235–39241.
Lyons, S.E., Lawson, N.D., Lei, L., Bennett, P.E., Weinstein, B.M., Liu, P.P., 2002. A nonsense mutation in zebrafish gata1 causes the bloodless phenotype in vlad tepes. Proc. Natl. Acad. Sci. U. S. A. 99, 5454–5459.
Magnusson, M., Brun, A.C., Lawrence, H.J., Karlsson, S., 2007a. Hoxa9/hoxb3/hoxb4 compound null mice display severe hematopoietic defects. Exp. Hematol. 35, 1421–1428.
Magnusson, M., Brun, A.C., Miyake, N., Larsson, J., Ehinger, M., Bjornsson, J.M., Wutz, A., Sigvardsson, M., Karlsson, S., 2007b. HOXA10 is a critical regulator for hematopoietic stem cells and erythroid/megakaryocyte development. Blood 109, 3687–3696.
Mann, R.S., 1995. The specificity of homeotic gene function. Bioessays 17, 855–863.
Mann, R.S., Affolter, M., 1998. Hox proteins meet more partners. Curr. Opin. Genet. Dev. 8, 423–429.
Mann, R.S., Chan, S.K., 1996. Extra specificity from extradenticle: the partnership between HOX and PBX/EXD homeodomain proteins. Trends Genet. 12, 258–262.
Maves, L., Waskiewicz, A.J., Paul, B., Cao, Y., Tyler, A., Moens, C.B., Tapscott, S.J., 2007. Pbx homeodomain proteins direct Myod activity to promote fast–muscle differentiation. Development 134, 3371–3382.
McKercher, S.R., Torbett, B.E., Anderson, K.L., Henkel, G.W., Vestal, D.J., Baribault, H., Klemsz, M., Feeney, A.J., Wu, G.E., Paige, C.J., Maki, R.A., 1996. Targeted disruption of the PU.1 gene results in multiple hematopoietic abnormalities. EMBO J. 15, 5647–5658.
McNulty, C.L., Peres, J.N., Bardine, N., van den Akker, W.M., Durston, A.J., 2005. Knockdown of the complete Hox paralogous group 1 leads to dramatic hindbrain and neural crest defects. Development 132, 2861–2871.
Mercader, N., Leonardo, E., Azpiazu, N., Serrano, A., Morata, G., Martinez, C., Torres, M., 1999. Conserved regulation of proximodistal limb axis development by Meis1/Hth. Nature 402, 425–429.
Minehata, K., Kawahara, A., Suzuki, T., 2008. meis1 regulates the development of endothelial cells in zebrafish. Biochem. Biophys. Res. Commun. 374, 647–652.
Moens, C.B., Selleri, L., 2006. Hox cofactors in vertebrate development. Dev. Biol. 291, 193–206.
Nakamura, T., Largaespada, D.A., Shaughnessy Jr., J.D., Jenkins, N.A., Copeland, N.G., 1996. Cooperative activation of Hoxa and Pbx1-related genes in murine myeloid leukaemias. Nat. Genet. 12, 149–153.
Nerlov, C., Querfurth, E., Kulessa, H., Graf, T., 2000. GATA-1 interacts with the myeloid PU.1 transcription factor and represses PU.1-dependent transcription. Blood 95, 2543–2551.
Orkin, S.H., 1992. GATA-binding transcription factors in hematopoietic cells. Blood 80, 575–581.
Orkin, S.H., Zon, L.I., 2008. Hematopoiesis: an evolving paradigm for stem cell biology. Cell 132, 631–644.
Patterson, L.J., Gering, M., Eckfeldt, C.E., Green, A.R., Verfaillie, C.M., Ekker, S.C., Patient, R., 2007. The transcription factors Scl and Lmo2 act together during development of the hemangioblast in zebrafish. Blood 109, 2389–2398.
Penkov, D., Di Rosa, P., Fernandez Diaz, L., Basso, V., Ferretti, E., Grassi, F., Mondino, A., Blasi, F., 2005. Involvement of Prep1 in the alphabeta T-cell receptor T-lymphocytic potential of hematopoietic precursors. Mol. Cell. Biol. 25, 10768–10781.
Pevny, L., Simon, M.C., Robertson, E., Klein, W.H., Tsai, S.F., D'Agati, V., Orkin, S.H., Costantini, F., 1991. Erythroid differentiation in chimaeric mice blocked by a targeted mutation in the gene for transcription factor GATA-1. Nature 349, 257–260.
Pineault, N., Buske, C., Feuring-Buske, M., Abramovich, C., Rosten, P., Hogge, D.E., Aplan, P.D., Humphries, R.K., 2003. Induction of acute myeloid leukemia in mice by the

human leukemia-specific fusion gene NUP98-HOXD13 in concert with Meis1. Blood 101, 4529–4538.
Popperl, H., Rikhof, H., Chang, H., Haffter, P., Kimmel, C.B., Moens, C.B., 2000. lazarus is a novel pbx gene that globally mediates hox gene function in zebrafish. Mol. Cell 6, 255–267.
Rekhtman, N., Radparvar, F., Evans, T., Skoultchi, A.I., 1999. Direct interaction of hematopoietic transcription factors PU.1 and GATA-1: functional antagonism in erythroid cells. Genes Dev. 13, 1398–1411.
Rhodes, J., Hagen, A., Hsu, K., Deng, M., Liu, T.X., Look, A.T., Kanki, J.P., 2005. Interplay of pu.1 and gata1 determines myelo-erythroid progenitor cell fate in zebrafish. Dev. Cell 8, 97–108.
Rieckhof, G.E., Casares, F., Ryoo, H.D., Abu-Shaar, M., Mann, R.S., 1997. Nuclear translocation of extradenticle requires homothorax, which encodes an extradenticle-related homeodomain protein. Cell 91, 171–183.
Ryoo, H.D., Marty, T., Casares, F., Affolter, M., Mann, R.S., 1999. Regulation of Hox target genes by a DNA bound Homothorax/Hox/Extradenticle complex. Development 126, 5137–5148.
Sarno, J.L., Kliman, H.J., Taylor, H.S., 2005. HOXA10, Pbx2, and Meis1 protein expression in the human endometrium: formation of multimeric complexes on HOXA10 target genes. J. Clin. Endocrinol. Metab. 90, 522–528.
Scott, E.W., Simon, M.C., Anastasi, J., Singh, H., 1994. Requirement of transcription factor PU.1 in the development of multiple hematopoietic lineages. Science 265, 1573–1577.
Shanmugam, K., Green, N.C., Rambaldi, I., Saragovi, H.U., Featherstone, M.S., 1999. PBX and MEIS as non-DNA-binding partners in trimeric complexes with HOX proteins. Mol. Cell. Biol. 19, 7577–7588.
Shen, W.F., Montgomery, J.C., Rozenfeld, S., Moskow, J.J., Lawrence, H.J., Buchberg, A.M., Largman, C., 1997a. AbdB-like Hox proteins stabilize DNA binding by the Meis1 homeodomain proteins. Mol. Cell. Biol. 17, 6448–6458.
Shen, W.F., Rozenfeld, S., Lawrence, H.J., Largman, C., 1997b. The Abd-B-like Hox homeodomain proteins can be subdivided by the ability to form complexes with Pbx1a on a novel DNA target. J. Biol. Chem. 272, 8198–8206.
Shen, W.F., Rozenfeld, S., Kwong, A., Kom ves, L.G., Lawrence, H.J., Largman, C., 1999. HOXA9 forms triple complexes with PBX2 and MEIS1 in myeloid cells. Mol. Cell. Biol. 19, 3051–3061.
Shimamoto, T., Tang, Y., Naot, Y., Nardi, M., Brulet, P., Bieberich, C.J., Takeshita, K., 1999. Hematopoietic progenitor cell abnormalities in Hoxc-8 null mutant mice. J. Exp. Zool. 283, 186–193.
Shivdasani, R.A., Mayer, E.L., Orkin, S.H., 1995. Absence of blood formation in mice lacking the T-cell leukaemia oncoprotein tal-1/SCL. Nature 373, 432–434.
Shivdasani, R.A., Fujiwara, Y., McDevitt, M.A., Orkin, S.H., 1997. A lineage-selective knockout establishes the critical role of transcription factor GATA-1 in megakaryocyte growth and platelet development. EMBO J. 16, 3965–3973.
Slape, C., Aplan, P.D., 2004. The role of NUP98 gene fusions in hematologic malignancy. Leuk. Lymphoma 45, 1341–1350.
So, C.W., Karsunky, H., Wong, P., Weissman, I.L., Cleary, M.L., 2004. Leukemic transformation of hematopoietic progenitors by MLL-GAS7 in the absence of Hoxa7 or Hoxa9. Blood 103, 3192–3199.
Stevens, K.E., Mann, R.S., 2007. A balance between two nuclear localization sequences and a nuclear export sequence governs extradenticle subcellular localization. Genetics 175, 1625–1636.
Stopka, T., Amanatullah, D.F., Papetti, M., Skoultchi, A.I., 2005. PU.1 inhibits the erythroid program by binding to GATA-1 on DNA and creating a repressive chromatin structure. EMBO J. 24, 3712–3723.
Vlachakis, N., Choe, S.K., Sagerstrom, C.G., 2001. Meis3 synergizes with Pbx4 and Hoxb1b in promoting hindbrain fates in the zebrafish. Development 128, 1299–1312.
Warren, A.J., Colledge, W.H., Carlton, M.B., Evans, M.J., Smith, A.J., Rabbitts, T.H., 1994. The oncogenic cysteine-rich LIM domain protein rbtn2 is essential for erythroid development. Cell 78, 45–57.
Waskiewicz, A.J., Rikhof, H.A., Hernandez, R.E., Moens, C.B., 2001. Zebrafish Meis functions to stabilize Pbx proteins and regulate hindbrain patterning. Development 128, 4139–4151.
Waskiewicz, A.J., Rikhof, H.A., Moens, C.B., 2002. Eliminating zebrafish pbx proteins reveals a hindbrain ground state. Dev. Cell 3, 723–733.
Williams, T.M., Williams, M.E., Innis, J.W., 2005. Range of HOX/TALE superclass associations and protein domain requirements for HOXA13:MEIS interaction. Dev. Biol. 277, 457–471.
Zhang, D.E., Hohaus, S., Voso, M.T., Chen, H.M., Smith, L.T., Hetherington, C.J., Tenen, D.G., 1996. Function of PU.1 (Spi-1), C/EBP, and AML1 in early myelopoiesis: regulation of multiple myeloid CSF receptor promoters. Curr. Top. Microbiol. Immunol. 211, 137–147.
Zhang, P., Behre, G., Pan, J., Iwama, A., Wara-Aswapati, N., Radomska, H.S., Auron, P.E., Tenen, D.G., Sun, Z., 1999. Negative cross-talk between hematopoietic regulators: GATA proteins repress PU.1. Proc. Natl. Acad. Sci. U. S. A. 96, 8705–8710.
Zhang, P., Zhang, X., Iwama, A., Yu, C., Smith, K.A., Mueller, B.U., Narravula, S., Torbett, B.E., Orkin, S.H., Tenen, D.G., 2000. PU.1 inhibits GATA-1 function and erythroid differentiation by blocking GATA-1 DNA binding. Blood 96, 2641–2648.